Since January 2020 Elsevier has created a COVID-19 resource centre with free information in English and Mandarin on the novel coronavirus COVID-19. The COVID-19 resource centre is hosted on Elsevier Connect, the company's public news and information website.

Structure *14*, 1293–1302, August 2006 DOI 10.1016/j.str.2006.06.012

Structural Basis of Ubiquitin Recognition by the Deubiquitinating Protease USP2

Martin Renatus,[1,*] Shirley Gil Parrado,[1] Allan D'Arcy,[1] Ulf Eidhoff,[1] Bernd Gerhartz,[1] Ulrich Hassiepen,[1] Benoit Pierrat,[1] Ralph Riedl,[1] Daniela Vinzenz,[1] Susanne Worpenberg,[1] and Markus Kroemer[2]
[1] Protease Platform
[2] Discovery Technologies
Novartis Institutes for BioMedical Research
4002 Basel
Switzerland

Summary

Deubiquitinating proteases reverse protein ubiquitination and rescue their target proteins from destruction by the proteasome. USP2, a cysteine protease and a member of the ubiquitin specific protease family, is overexpressed in prostate cancer and stabilizes fatty acid synthase, which has been associated with the malignancy of some aggressive prostate cancers. Here, we report the structure of the human USP2 catalytic domain in complex with ubiquitin. Ubiquitin uses two major sites for the interaction with the protease. Both sites are required simultaneously, as shown by USP2 inhibition assays with peptides and ubiquitin mutants. In addition, a layer of ordered water molecules mediates key interactions between ubiquitin and USP2. As several of those molecules are found at identical positions in the previously solved USP7/ubiquitin-aldehyde complex structure, we suggest a general mechanism of water-mediated ubiquitin recognition by USPs.

Introduction

Posttranslational modification with ubiquitin regulates protein stability and localization and is crucial for homeostasis of eukaryotic cells. In a multistep process involving three classes of enzymes called E1 (ubiquitin activating), E2 (ubiquitin conjugating), and E3 (ubiquitin ligating), an isopeptide bond is formed between the C-terminal group of ubiquitin and a lysine ε-amino group of the targeted protein. Ubiquitination is reversed by a number of proteases that specifically recognize ubiquitinated proteins and remove the ubiquitin tag by hydrolyzing the isopeptide bond. Currently almost 100 putative deubiquitinating proteases (DUBs; or ubiquitin-specific processing proteases UBP) belonging to 5 distinct families are known (Amerik and Hochstrasser, 2004; Nijman et al., 2005), the majority of which are cysteine proteases, including 4 human ubiquitin C-terminal hydrolyases (UCHs) and 54 human ubiquitin-specific proteases (USPs). USPs are multidomain proteases that vary in size and complexity but share a certain degree of homology within their catalytic units, namely within three regions termed the Cys-, His-, and QQD-Box (Quesada et al., 2004). In most USPs, the catalytic unit is preceded and followed by additional domains that are believed to determine subcellular localization and substrate recognition. Little is known about the physiological function of most human USPs, and specific substrates often remain elusive. A well-studied example is USP7 (HAUSP), which stabilizes both p53 and mdm2, thereby playing an important role in the p53 pathway (Li et al., 2002, 2004; Cummins et al., 2004; Cummins and Vogelstein, 2004). Several publications describe the structural basis for substrate recognition by USP7 (Hu et al., 2002, 2006; Sheng et al., 2006).

Less is known about the structure and function of USP2. It is overexpressed in human prostate cancer and prolongs the half-life of fatty acid synthase (Graner et al., 2004), a metabolic enzyme associated with the malignancy of aggressive prostate cancer (Baron et al., 2004). In addition, USP2 itself has oncogenic properties in vivo and in vitro that are linked to its proteolytic activity (Priolo et al., 2006). Mdm2 appears to be another substrate for USP2, indicating that USP2 also plays a role in the regulation of the p53 pathway (L.F. Stevenson et al., submitted).Together, these data provide a first rationale for USP2-directed therapies in the treatment of prostate cancer. A possible strategy is the inhibition of its proteolytic activity.

To aid the discovery of active site-directed inhibitors, we solved the three-dimensional structure of USP2 in complex with ubiquitin at a resolution of 1.85 Å. We suggest a general mode of substrate recognition by USPs, where conserved water molecules mediate interactions between the ubiquitin core (residues *1–71*) and the protease. The five C-terminal residues of ubiquitin (*Arg72-Leu73-Arg74-Gly75-Gly76*) bind into the active site cleft without making covalent interactions with the active site cysteine. Kinetic studies with peptidic substrates and truncated ubiquitin mutants show that neither the C-terminal peptide nor ubiquitin deletion mutants lacking the C-terminal residues bind to USP2 with detectable affinity.

Results

Overall Structure of the USP2/Ubiquitin Complex

USP2 is reported to exist in several isoforms (http://merops.sanger.ac.uk/), and it is unclear how these differ in function. The isoforms consist of an N-terminal region of variable length and a 347 amino acid large C-terminal domain. The C-terminal domain possesses the sequence signatures of an USP catalytic domain (Figure 1). In the largest isoform, USP2a, the catalytic domain is preceded by 258 amino acids, in the shortest by only 6. We focused our studies on the conserved catalytic domain. For clarity, the construct comprising residues 259–605 will hereon be referred to as USP2. USP2 was produced with high yields as recombinant protein in *E. coli*, and it cleaved the synthetic substrate ubiquitin-AMC with a catalytic efficiency k_{cat}/K_M of 2.6×10^5 $M^{-1}s^{-1}$ (Table 1). To facilitate the comparison of key residues, we refer the numbering of USP2 to that of USP7 (Figure 1), for which the first USP structure was published (Hu et al., 2002).

*Correspondence: martin.renatus@novartis.com

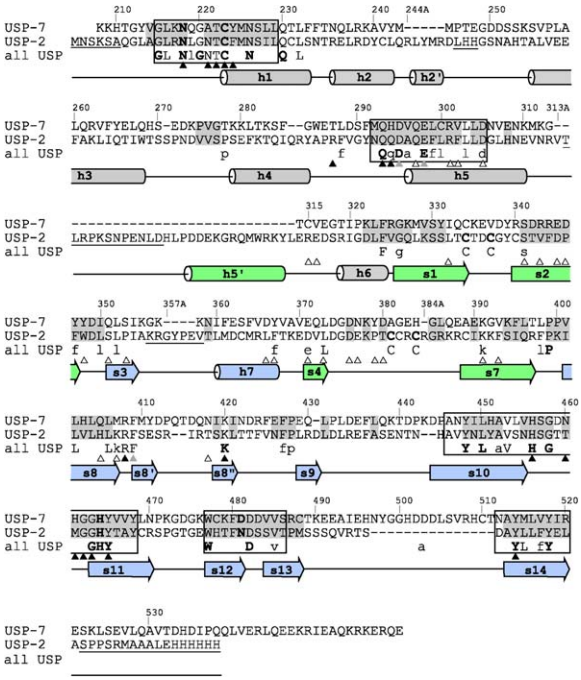

Figure 1. Structure-Based Sequence Alignment of the Human USP2 and USP7 Catalytic Domains

Cα positions that are in a structural alignment within 1.7 Å are highlighted by gray boxes. USP2 residues are numbered according to the corresponding USP7 residues; insertion loops in USP2 relative to USP7 are numbered alphabetically. Active-site residues (catalytic triad: Cys223, His464, Asp/Asn481; and oxyanion hole: Asn218) and the four cysteine residues (Cys334, Cys337, Cys381, Cys384) coordinating a metal ion are shown in bold. USP2 residues poorly defined by electron density are underlined. Secondary structure elements are colored as in Figure 2B (thumb, gray; fingers, lime; palm, blue). Forty-seven USP2 residues that are within 4 Å of ubiquitin are denoted by triangles. Open triangles, interactions with the ubiquitin core (ubiquitin residues *1–71*); solid black triangles, interactions with the ubiquitin C terminus (ubiquitin *72–76*); solid gray triangles, interactions with both ubiquitin core and C terminus. A consensus sequence, based on the alignment of 54 human USPs (Quesada et al., 2004) and denoted as "all USP," is included in the alignment (bold capital letters, identical in more than 90% of the sequences; capital letters, identical in more than 80% of the sequences; small letters, identical in more than 60% of the sequences). Regions of high sequence conservation within the human USPs are highlighted with boxes: Cys-box (215–229), QDE-box (292–305), and His-box (446–468, 477–486, and 512–520).

Despite repeated trials with numerous USP2 preparations, we failed to crystallize ligand-free USP2. This might be due to the strong tendency of USP2 to aggregate, which is highly accelerated at temperatures below 10°C. Interestingly, complexation of USP2 with ubiquitin-aldehyde (resulting in a covalent complex) or unmodified ubiquitin (resulting in a noncovalent complex) prevented aggregation and yielded crystals that grew overnight. Analysis by SDS-PAGE showed that the crystals contain both protein components, USP2 and ubiquitin (data not shown). Diffraction properties improved significantly upon dehydration of the crystals (Abergel, 2004), and a data set with 1.85 Å resolution was obtained. The structure could be solved by molecular replacement with USP7 as search molecule.

The USP2 structure contains nine α helices and 14 β strands (Figure 2A). Its overall shape resembles a cupped hand with the approximate dimensions of 35 Å × 40 Å × 65 Å and comprises three domains termed thumb, palm, and fingers (Figure 2B), an analogy first used for USP7 (Hu et al., 2002). The finger domain is formed by a four-stranded β sheet (s1, s2, s4, s7), which is flanked by helix h5′. This helix is absent in USP7, while two short strands at the tip of the fingers, present in USP7 (s5 and s6), are missing in USP2 (Figure 2C). The thumb is formed by seven helices (h1–h6, including h5′). Compared to USP7, it lacks two additional C-terminal helices (h9 and h10). The palm connects fingers and the thumb and is formed by several β strands and α helices (s3, s8–s14, h7, and h8). Residues 214–229 (Cys-box) and 292–305 (QDE-box) of the thumb, as well as residues 446–486, 477–486, and 512–520 of the palm (His-box), form the active site (Quesada et al., 2004). The conserved residues Cys223, His464, and Asn481 form the catalytic triad, and Asn218 the oxyanion hole (http://merops.sanger.ac.uk/). The cupped hand of USP2 nicely accommodates ubiquitin, an 8 kDa small and spherical molecule with a diameter of approximately 25 Å. In the complex, 3850 Å^2 of the solvent-accessible surface is buried, which corresponds to roughly 40% of the ubiquitin surface. USP2 and ubiquitin have complementary shapes, providing a first structural explanation for the high selectivity of USPs for ubiquitin substrates.

Metal Binding Site

In USP2, a metal binding site is located between the two loops connecting strands s1–s2 and s4–s7, where four cysteine residues (Cys334, Cys337, Cys381, Cys384) coordinate a metal ion (Figure 2A). The corresponding Sγ-metal ion distances are 2.46 Å, 2.38 Å, 2.40 Å, and 2.47 Å, close to the reported ideal distance (2.35 ± 0.09 Å) for structural zinc binding sites in proteins

Table 1. Steady-State Kinetic Parameters for the Hydrolysis of AMC Substrates by UCH-L3 and USP2

	USP2			
	K_M (M)	k_{cat} (s^{-1})	k_{cat}/K_M (M^{-1} s^{-1})	[Enz] (M)
Ubiquitin-AMC	554×10^{-9}	0.14	252×10^{3}	1.5×10^{-9}
Ac-RLRGG-AMC	inactive	inactive	inactive	1.0×10^{-6}
Ac-HLVLRLRGG-AMC	inactive	inactive	inactive	1.0×10^{-6}
	UCH-L3			
	K_M (M)	k_{cat} (s^{-1})	k_{cat}/K_M (M^{-1} s^{-1})	[Enz] (M)
Ubiquitin-AMC	32×10^{-9}	7.34	229×10^{6}	3.0×10^{-12}
Ac-RLRGG-AMC	3.0×10^{-4}	7.6×10^{-6}	2.5×10^{-2}	5.0×10^{-7}
Ac-HLVLRLRGG-AMC	7.3×10^{-5}	1.8×10^{-5}	2.5×10^{-1}	6.0×10^{-7}

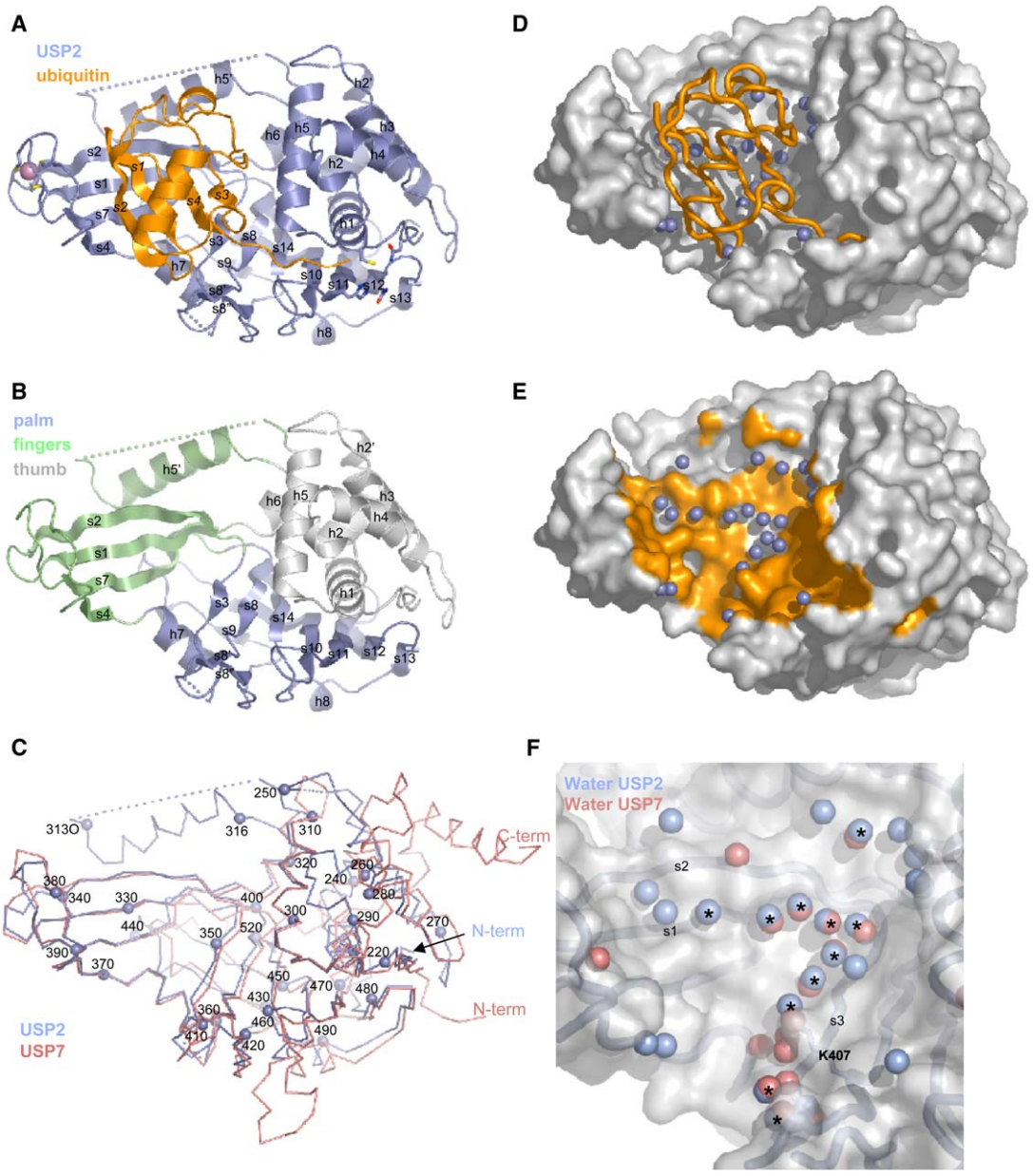

Figure 2. The X-Ray Structure of the USP2 Catalytic Domain in Complex with Ubiquitin

The catalytic domain consists of residues 259–605 of full-length USP2. Secondary structure elements are named according to the USP7 structure (Hu et al., 2002). The loops connecting h5 and h5′ as well as s3 and h7 are poorly defined by electron density (see also Figure 1) and are therefore omitted from the final model. Dotted lines highlight these gaps.

(A) Overall structure of the USP2/ubiquitin complex (blue/orange ribbon). The active-site residues Asn218, Cys223, His464, and Asn481 as well as the metal binding site Cys334, Cys337, Cys381, and Cys384 are shown as sticks, and the zinc ion is shown as a pink sphere.

(B) Overall structure of USP2. Secondary elements forming the palm, the fingers, and the thumb are painted in blue, lime, and gray, respectively. Ubiquitin has been omitted for clarity.

(C) Superposition of the catalytic domain of USP2 in blue with the catalytic domain of USP7 in salmon (1BNF). The ubiquitin molecules of both complex structures superimpose perfectly and have been omitted for clarity.

(D) Solvent molecules (blue) mediate the binding of ubiquitin (orange) to USP2 (gray surface).

(E) Solvent molecules mediating the binding of ubiquitin are shown as blue spheres, and the molecular surface corresponding to USP2 residues within 4.0 Å of the ubiquitin molecule is highlighted in orange. The ubiquitin molecule has been omitted for clarity.

(F) Superimposition of buried water molecules (USP2/ubiquitin, blue; USP7/ubiquitin-aldehyde, salmon). Stars highlight equivalent water positions. USP2 is shown as a gray transparent surface. Lys407 of USP2, replacing a water molecule present in the USP7/ubiquitin-aldehyde structure, is shown as sticks.

(Alberts et al., 1998). Based on these distance criteria and on a MAD experiment (see Supplemental Data), we conclude that this metal ion is a tightly bound zinc ion. This CXXC-X_n-CXXC metal binding motif is common among USPs (Krishna and Grishin, 2005). Of 54 (Quesada et al., 2004) putative human USPs, the motif is

absent only in USP5, USP7, USP10, USP13, USP14, USP25, USP28, USP34, and USP39. Also the viral protease SARS-CoV PLpro, which has deubiquitinating activity and is structurally similar to human USPs (Ratia et al., 2006), contains an intact zinc binding site at the homologous position. The two CXXC sequence patterns are mostly separated by approximately 50 residues, although in some cases (e.g., USP4 and USP6), an additional domain of up to 350 amino acids is inserted at this position. Based on the structure of human USP7, it has been predicted that the finger domain of USPs is a zinc ribbon (Krishna and Grishin, 2005), a structure module that is known to serve as an interaction domain in many proteins. Krishna and Grishin hypothesized that the zinc ribbon domain has been inserted into a papain-like protease domain, the ancestor of USPs, to serve as a scaffold for ubiquitin recognition. In some USPs, including USP7, several of the four cysteine residues have been mutated during evolution, and the zinc binding ability was lost while the fold was maintained. This indicates that a metal binding site is not required for deubiquitinating activity. Therefore, the precise function of the zinc binding site in USP2 and other USPs remains elusive.

Specific Interactions of USP2 with Ubiquitin

The structure shows USP2 in a noncovalent complex with ubiquitin. Ubiquitin uses two sites for the interaction with USP2. Its core (residues *1–71*; throughout the paper ubiquitin residues are given in italics, USP2 residues in normal font) binds into the cupped hand contacting residues of all three structural elements, fingers, thumb, and palm, while its five C-terminal residues (*72–76*) bind into a narrow channel and reach for the active site cysteine (Figure 2D). As many as 30 USP2 residues are within 4 Å of the ubiquitin core. Among those, 12 are engaged in H bond and salt bridge interactions: 5 are found at the tip of the fingers (Ser341, Asp345, Asp371, Asp376, Glu377), involving ubiquitin residues from strands *s1* and *s2* and from the loop preceding strand *s4*. The others are located on the thumb (Asp295, Glu298, Arg301, Glu316, Lys407, Thr418) and palm (Leu366), interacting with the ubiquitin residues following strands *s1* and *s4* and the ones preceding *s3*. However, for a significant fraction of the total contact area the interactions are indirect, as numerous solvent molecules mediate H bond interactions between ubiquitin backbone and USP2 side chain/backbone atoms (Figures 2D and 2E). In total, 25 solvent molecules are located in the region between the tip of the fingers and the thumb, and most of them are lined up along strands s1, s2, and s3 (Figure 2F).

The C terminus of ubiquitin *Arg72-Leu73-Arg74-Gly-75-Gly76* binds with its *Gly-Gly* motif into a narrow channel reaching for the active site cysteine (Figure 2D). The backbone atoms of *Leu73*, *Arg74*, and *Gly75* form a network of six H bonds with USP2 (Figure 3A). The side chain of *Arg74* is solvent accessible, while *Leu73* binds into a hydrophobic pocket and the guanidinium group of *Arg72* interacts with Glu298. No nearby countercharge neutralizes the negative charge of the ubiquitin carboxyl terminus. Instead, three H bond interactions with Cys223N, Asn221Nδ2, and Gln293Nε2 stabilize the C terminus in its conformation. The negative

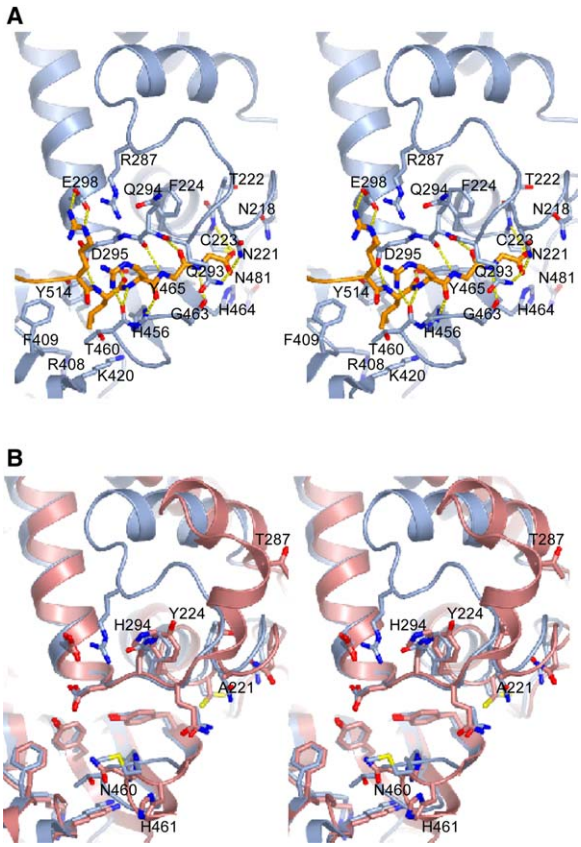

Figure 3. Substrate Binding Region of USP2 and USP7

(A) USP2/ubiquitin complex: the five C-terminal residues of ubiquitin, *Leu-Arg-Leu-Gly-Gly*, are shown as orange sticks. USP2 side chains that are within 4.0 Å of the ligand as well as residues Asn218, His464, and Asn481 of the active site are shown as sticks. Putative hydrogen bonds are indicated by yellow dotted lines.

(B) Superimposition of the binding region of USP2 (blue) and USP7 (salmon): residues forming the substrate recognition pocket for the ubiquitin C terminus as well as the catalytic Cys223 are shown as sticks. Only USP7 residues that differ from USP2 are labeled.

charge of the *Gly76* carboxy group does not seem to be well balanced in the complex, especially as the Cys223 Sγ atom is most likely deprotonated (see Discussion), leading to electrostatic repulsion between the two negatively charged moieties. Indeed, the side chain of Cys223 seems to exist in two rotamers: a small population adopts the catalytically active conformation, which was observed in the USP7/ubiquitin-aldehyde complex (Figure 3B), as suggested by a very weak difference electron density peak. Mostly, Cys223 is rotated by 120° with Sγ pointing away from ubiquitin *Gly76* and in the direction of Asp482 (Figure 3B). The electron density of Asp482 is rather poor, although all neighboring side chains are well defined, indicating increased mobility.

Comparison of Ubiquitin Binding to USP2 and USP7

Despite a limited sequence identity of ~24%, the overall fold of the USP2 and USP7 catalytic domains is conserved. The two structures superimpose with an rmsd of 1.25 Å for 262 Cα positions, which corresponds to 75% of the USP2 residues (Figures 1 and 2C). A similar

structural identity exists between USP2 and USP14, where 256 Cα positions can be aligned with an rmsd of 1.43 Å. However, as the USP14/ubiquitin-aldehyde complex (Hu et al., 2005) has been solved at significantly lower resolution than the corresponding complex with USP7 (3.5 Å versus 2.3 Å), we focus in our structural comparison on USP7. Structural elements that directly interact with ubiquitin, namely the base of the fingers and the surroundings of the active site, superimpose especially well, ensuring conservation of ubiquitin binding. Indeed, the 76 ubiquitin Cα positions of the USP2 and USP7 complexes differ with an rmsd of only 0.74 Å. This high structural similarity shows that the different protocols for the preparation of USP/ubiquitin complexes have no influence on the overall ubiquitin binding mode. Ubiquitin was used for the USP2/ubiquitin complex, while ubiquitin-aldehyde was used for the formation of corresponding USP7 complex. Ubiquitin-aldehyde is a chemically modified form of ubiquitin and highly potent USP inhibitor, where the terminal carboxy group has been reduced to an aldehyde for increased electrophilicity and affinity. In the resulting USP/ubiquitin-aldehyde complex, a covalent bond between inhibitor and protease is formed, representing a classical transition state mimetic for cysteine protease substrate complexes (Westerik and Wolfenden, 1972). Therefore, the USP7/ubiquitin-aldehyde and the USP14/ubiquitin-aldehyde complex structures reveal how USPs stabilize the tetrahedral intermediate ("oxyanion") that is formed during catalysis. Instead, no covalent bond is formed in the USP2/ubiquitin complex. The structure represents the noncovalent protease/product complex, the last step of peptide cleavage catalyzed by proteases. As such, it can help explain the structural reasons for substrate inhibition, a phenomenon that is observed in this class of enzymes (see below).

Most USP residues that interact directly with ubiquitin, both with the ubiquitin core (*1–71*) and the C terminus (*72–76*), are conserved (Figure 1). The binding clefts in USP2 and USP7 for the ubiquitin C terminus are almost identical. Only the loop around position 287 adopts different conformations. Of the 20 USP residues that are within 4 Å of the ubiquitin C-terminal penta-peptide, 14 are conserved, while residues at position 221, 224, 287, 294, 460, and 461 differ in sequence (Figure 3B). All of these six amino acid exchanges except for the one at position 221 (Asn in USP2, Ala in USP7) most likely have no influence on the ubiquitin binding. The significance of the exchange at position 221 is difficult to rationalize, especially as this residue is highly conserved in the USP family of proteases. In 42 USPs, including USP2, USP5, and USP14, an asparagine is found at this position, and in only six USPs, including USP7, an alanine is found. In the USP2/ubiquitin complex, Asn221 Nδ is in close contact to one oxygen of the *Gly76* carboxylate, while Asn218 Nδ ("oxyanion hole") interacts with the second C-terminal oxygen, an interaction similar to the one observed in the USP7/ubiquitin-aldehyde complex. Therefore, Asn221 together with Asn218 contributes to the stabilization of the negative charge on the ubiquitin C terminus (Figure 3A). In the USP14/ubiquitin-aldehyde complex, where the ubiquitin C terminus is covalently bound to the site cysteine and only one C-terminal oxygen is present, Asn108 (Asn218 in USP2) interacts with the hydroxyl of the thiohemiacetal, while Asn111 (Asn221 in USP2) makes no specific interactions and is rotated away from the active site. This comparison indicates that Asn221 plays a role, not in the stabilization of the transition state during catalysis, but rather in the stabilization of the enzyme product. This way, Asn221 might contribute to product inhibition (see below), and the high conservation of this residue suggests this characteristic is shared by most USPs. Unfortunately, so far, the catalytic properties of only one other member of the USP family, USP5 or isopeptidase T, has been characterized extensively (Stein et al., 1995). Also, USP5 has an asparagine at the corresponding position and is inhibited by ubiquitin. The question whether USPs, such as USP7, that don't have an asparagine at this position bind ubiquitin with lower affinity and show less substrate inhibition remains open until a detailed enzymatic characterization of these enzymes becomes available.

USP residues interacting with the ubiquitin core are in general poorly conserved (Figure 1), with the exception of 12 USP2 residues (see above) that are engaged in direct polar interactions. Among these 12 residues, 7 are conserved. Of the 5 nonconserved residues, 2 interact via their main-chain atoms (Leu366, Glu377), and only 3 (Glu316, Lys407, Thr418) are involved in interactions that are not possible in USP7. Overall, the same mode of ubiquitin recognition has been observed for USP14 (Hu et al., 2005). Based on the structural data and sequence conservation, it can be predicted that functional USPs share not only the overall structure but also use the described determinants for ubiquitin recognition and binding.

Inhibition of USP2 by Ubiquitin and Ubiquitin Truncation Mutants

After having shown that ubiquitin interacts with USP2 by using two sites, we tried to determine the individual contribution of the isolated interactions to the ubiquitin binding affinity. To this end, we first generated ubiquitin and three C-terminally truncated mutants (ubiquitin *1–74*, ubiquitin *1–73*, and ubiquitin *1–72*) in *E. coli* as reagents for enzymatic inhibition assays. The heterologously expressed proteins were characterized by ^{1}H-NMR spectroscopy and differential scanning calorimetry, by using endogenous ubiquitin purified from bovine thymus as a reference. The reference sample as well as all recombinant-expressed protein samples unfolded in a cooperative manner with the transition temperatures, Tm, in a similar range. The measured Tm's were 98.3°C (reference sample, endogenous ubiquitin), 91.9°C (ubiquitin), 91.9°C (ubiquitin *1–74*), 90.7°C (ubiquitin *1–73*), and 98.2°C (ubiquitin *1–72*), indicating that the C-terminal truncations have no major influence on protein stability. The ^{1}H NMR spectra of the endogenous and recombinant ubiquitin are largely identical. In addition, truncated mutants show only minor differences compared to the reference (data not shown). Taken together, these results indicate that heterologous expression of ubiquitin in *E. coli* yields a properly folded protein and that C-terminal truncations do not disturb the structure of the ubiquitin core. As an additional control experiment, we measured a K_i of 0.27 μM for the

Table 2. Inhibition of USP2

Inhibitor	K_i (M)
Ubiquitin[a]	$2.8 \pm 0.14 \times 10^{-6}$
Ubiquitin 1–74[b]	$1.0 \pm 0.09 \times 10^{-6}$
Ubiquitin 1–73[c]	$>1 \times 10^{-4}$
Ubiquitin 1–72[d]	$>1 \times 10^{-4}$
Ubiquitin 1–71[e]	$>1 \times 10^{-4}$
Ac-HLVLRLRGG-OH[f]	$>1 \times 10^{-4}$

[a] Full-length ubiquitin.
[b] Truncation mutants lacking *Gly75-Gly76*.
[c] Truncation mutants lacking *Arg74-Gly75-Gly76*.
[d] Truncation mutants lacking *Leu73-Arg74-Gly75-Gly76*.
[e] Truncation mutants lacking *Arg72-Leu73-Arg74-Gly75-Gly76*.
[f] Ubiquitin C-terminal peptide.

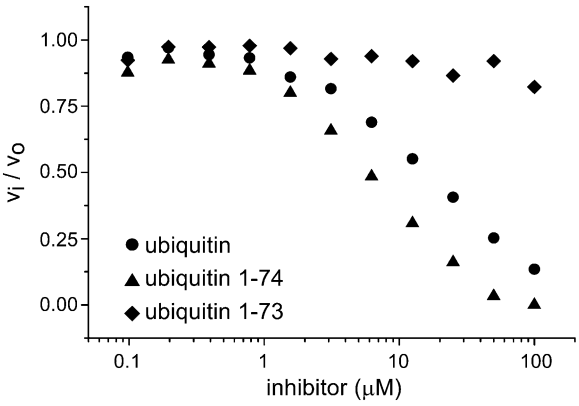

Figure 4. USP2 Inhibition by Full-Length Ubiquitin and the C-Terminally Truncated Mutants, Ubiquitin *1-74* and *1-73*

Residual enzymatic activity was determined at 22°C with ubiquitin-AMC as substrate. The relative activity (v_i/v_o) is plotted against the inhibitor concentration. From these data, the corresponding K_is were deduced as described in the Experimental Procedures section. The assay was performed in triplicate; the figure shows one representative set of measurements.

inhibition of UCH-L3 by ubiquitin with the substrate ubiquitin-AMC. This K_i is close to the published value of 0.3 μM (Wilkinson et al., 1999), which further validates the experimental setup. Next, by using the same assay format, the influence of ubiquitin on the proteolytic activity of USP2 was analyzed. USP2 is inhibited by ubiquitin with a K_i of 2.8 μM, which is in the same range as the K_i of 3 μM for the related enzyme USP5, also known as isopeptidase T (Dang et al., 1998). This shows that USP2 binds ubiquitin with significant affinity, and it suggests that product inhibition by ubiquitin is a general feature of the USP family of proteases. The biological significance of product inhibition is unknown. It might play a role in the regulation of USP activity, as with increasing intracellular ubiquitin concentration the deubiquitinating activity might be reduced. Yet, such an inhibition will only be observed if the concentration of free ubiquitin is in the same range as the K_d for the interaction between ubiquitin and the protease.

The structure of the USP2/ubiquitin complex shows that ubiquitin uses two interaction sites: its core (residues *1–71*) binds into the cupped hand interacting with fingers and palm, and its C terminus (residues *72–76*) binds into the substrate cleft at the catalytic center. To determine the contribution of each binding site to the total affinity, we analyzed the two binding events independently. The contribution of the C-terminal peptide was assessed by measuring the Michealis-Menten parameters for two peptidic AMC substrates, consisting of the last five and nine ubiquitin C-terminal residues, respectively. Neither of the substrates is cleaved by USP2 under the assay conditions (Table 1). This observation does not result from an unfavorable substrate conformation, as UCH-L3 is able to cleave both Ac-RLRGG-AMC and Ac-HLVLRLRGG-AMC, although with significantly lower catalytic efficiency compared to ubiquitin-AMC, but rather indicates that substrates do not bind to USP2. This interpretation is further supported by an additional inhibition experiment showing that the C-terminal peptide Ac-HLVLRLRGG has no effect on the proteolytic activity of USP2 (Table 2). Next, the contribution of the ubiquitin core to the total binding affinity was analyzed. The truncation mutants ubiquitin *1–72* and *1–73* affect the proteolytic activity of USP2 only marginally even at the highest inhibitor concentration used (Figure 4), indicating that the K_i for these mutants is significantly higher then 100 mM. In summary, our data show that the ubiquitin core and the ubiquitin C terminus alone bind USP2 very weakly with affinities at best in the high micromolar range, while full-length ubiquitin inhibits USP2 with a K_i of 2.8 μM.

Discussion

USP2 is one of 54 human members of the family of ubiquitin-specific proteases (USPs). USPs belong to the clan CA of papain-like proteases (http://merops.sanger.ac.uk/), which are characterized by catalytic residues in the order Cys, His, Asp/Asn in sequence, with the active site cysteine located at the beginning of a central α helix. Despite large sequence and structural divergence among the different representatives of this clan, the residues of the catalytic triad superimpose well (Johnston et al., 1997; Hu et al., 2002). Therefore, it has been suggested that members of clan CA share the catalytic mechanism with the active site cysteine and histidine residues forming a thiolate-imidazolium ion pair (Storer and Menard, 1994). Mutagenesis studies on USP7 (Hu et al., 2002) corroborate the importance of these residues for the catalytic activity of USPs. Yet, USPs differ fundamentally from other papain-like proteases as they require ubiquitin to reach full catalytic activity. While USP5 cleaves ubiquitin-derivatized substrates at rates close to diffusion control, short peptidic substrates containing the C-terminal residues of ubiquitin are turned over at significantly lower rates (Stein et al., 1995). In addition, ubiquitin binds to and inhibits USP5. The structures of USP7 in the absence and presence of ubiquitin-aldehyde gave a first structural explanation for the high substrate selectivity of USPs (Hu et al., 2002). Only when ubiquitin is bound does the enzyme adopt a catalytic-competent conformation. In the absence of ubiquitin, active-site residues and residues delineating the substrate binding sites are misaligned. Yet, as the structural rearrangements are restricted to the vicinity of the active site, where the C-terminal residues

of ubiquitin bind, it remained unclear why short peptides mimicking the ubiquitin C terminus are poor USP substrates.

In line with the data published for USP5 (Stein et al., 1995), we show that USP2 turns over ubiquitin-AMC with a high catalytic efficiency (k_{cat}/K_M of 2.5×10^5 $M^{-1}s^{-1}$), while it is unable to cleave peptidic AMC substrates consisting of five or nine amino acids from the ubiquitin C terminus. At first sight, these results suggest that the core of ubiquitin and not its C terminus are required for the binding to USP2. Consequently, the main contribution for the binding affinity results from interactions between the ubiquitin core (residues *1–71*) and the USP2 fingers and palm domains. To test this hypothesis, several C-terminal-truncated ubiquitin mutants were analyzed in USP2 inhibition assays. While ubiquitin inhibits USP2 with a K_i of 2.8 μM, mutants lacking residues *Arg74-Gly75-Gly76* or *Leu73-Arg74-Gly75-Gly76* affect the proteolytic activity of USP2 only marginally even at the highest inhibitor concentration. In summary, the interactions between the ubiquitin core and the fingers/palm as well as the one between the ubiquitin C terminus and the active site cleft are very weak, and both interactions are required simultaneously for ubiquitin binding. The weak affinities of the C-terminal ubiquitin peptides together with the methods available in the kinetic analysis do not allow the determination of the exact K_i values for the inhibition of USP2. Therefore, it remains unknown whether the binding to the two low-affinity sites is cooperative or purely additive. Yet, cooperative binding seems likely: based on the analogy to USP7, we assume that prior to ligand binding, the active site of USP2 is in a catalytically incompetent conformation. In this conformation, the two active-site residues cysteine and histidine are too far apart to form a catalytic diad, and the substrate binding site at the catalytic center is absent. When ubiquitin binds to USP2, its core is recognized by the cupped hand. This interaction aligns the ubiquitin C terminus into the right orientation and register, so that it can bind to the active site cleft and induce the active conformation of the enzyme. Isolated C-terminal fragments cannot be prealigned. Therefore they bind with very low affinity and are unable to induce an active conformation. For the design of low molecular weight active-site-directed inhibitors of USP2, these findings suggest that, in order to gain potency, the ligand has to bind in such an induced-fit binding mode. This might only be achievable if the inhibitor spans both interaction sites.

Interestingly, a ubiquitin mutant lacking *Gly75-Gly76* is a slightly more potent USP2 inhibitor than full-length ubiquitin (K_i of 1.0 μM versus 2.8 μM). This suggests that the two C-terminal ubiquitin residues make no significant net contribution to the USP2/ubiquitin interaction. This is surprising, as, in the USP2/ubiquitin complex structure, the *Gly75-Gly76* dipeptide binds into a narrow channel formed by the highly conserved residue Gln293 and is engaged in five potential H bond interactions. A possible explanation is the charge-charge repulsion between the negatively charged *Gly76* carboxylate and the Cys223 $S\gamma$, which we assume to be negatively charged based on the analogy to papain (see above). This repulsion leads to the observed reorientation of Cys223 and the destabilization of the protease/ligand complex. By contrast, in a putative USP2/ubiquitin *1–74* complex, the distance between the two negative charges is increased by at least 7 Å. At this distance, the repulsion between the ubiquitin C terminus and the USP2 active-site cysteine is reduced. The interaction is strengthened, and the loss of the five potential H bonds more than compensated.

Based on the USP7 (Hu et al., 2002) and USP14 (Hu et al., 2005) structures, it has been predicted that the overall fold is conserved among USPs. Despite significant variations between different USP sequences, several elements required for ubiquitin recognition are allegedly shared by functional USPs. Most of these elements are found in USP2 as well. Yet, besides conservation of key residues at the tip of the fingers, residues forming the binding site for the ubiquitin core are diverse in the USP family, namely between USP2 and USP7 (Figure 1). Still, USP2 and USP7 bind ubiquitin in the same way. In the absence of sequence conservation, the interactions between ubiquitin and the USP are conserved by a layer of water molecules. Eleven of these water molecules are found at identical positions in the USP2 and USP7 complexes (Figure 2F). They are placed along strands s1, s2, and s3, regions of diverse sequence, and mediate H bond interactions between ubiquitin and main-chain atoms of USP2. The conservation of specific USP/ubiquitin interactions in the absence of sequence conservation is illustrated by the interactions with ubiquitin *Lys6* carbonyl oxygen. In the USP2/ubiquitin complex, $N\zeta$ of Lys407 occupies the same position as a solvent molecule in the USP7/ubiquitin-aldehyde complex.

The principles of protein-protein interactions and the role of water molecules in molecular recognition have been studied by various groups (Janin, 1997; Jones and Thornton, 1996; Larsen et al., 1998). "Wet" protein-protein interfaces where a large fraction of interactions are water mediated are not uncommon but are less abundant then complexes where the contact interface is largely dehydrated (Janin, 1997). For example, water-mediated interactions have been reported for the L-arabinose binding protein (Quiocho et al., 1989), the barnase-barstar complex (Buckle et al., 1994), and the *Streptomyces griseus* protease B-ovomucid complex (Huang et al., 1995). The contribution of water-mediated interactions to the binding affinity is difficult to assess both experimentally and theoretically (Rodier et al., 2005). In general, hydrophobic interactions are tighter than polar interactions (Tsai et al., 1997), while water-mediated and direct polar interactions are believed to be of similar strength (Rodier et al., 2005). The USP2-ubiquitin interface in the area of the ubiquitin core (*1–71*) appears to be less hydrophobic than protease-inhibitor interfaces in general. This is no surprise, as ubiquitin has to dissociate from USP2 once it is cleaved off its target protein and should not act as a tight inhibitor. In the USP-ubiquitin complexes, the solvent molecules fill parts of the cavity formed at the protein-protein interface and act as a coating that prevents the two molecules from interacting directly. They provide specific, conserved interaction sites. We hypothesize that this mode of substrate recognition is common to all USPs and that mediating water molecules will also be found in other USP/ubiquitin complexes.

Experimental Procedures

USP2 and UCH-L3 Preparation

The boundaries of the catalytic domain of human USP2 have been defined by aligning different USP2 isoforms and orthologs. The catalytic core, Asn259 to Met605, was amplified by PCR from a cDNA encoding for full-length human USP2 (UniProt ID O75604) with the sense 5′-CTGAATTCGGATCCGCCGCCATGGCACATATGAATTC TAAGAGTGCCCAG-3′ and the antisense primer 5′-GACTCGAGT TACTATGCGGCCGCCATTCGGGAGGGCGGGCTG-3′ into a modified pET24a vector (Novagen) in frame with the C-terminal His tag by using the restriction enzymes NdeI/NotI.

E. coli strain Rosetta (DE3)pLysS harboring the human USP2 expression plasmid was cultivated at 37°C in LB medium (30 μg/ml kanamycin, 34 μg/ml chloramphenicol) and induced at an OD_{600} of 0.5–0.8 with 0.5 mM IPTG. After 2–5 hr of induction, the cells were harvested by centrifugation and frozen at −20°C. Cells from a 4 liter *E. coli* cell culture were resuspended in 200–300 ml buffer A (10 mM Tris/HCl [pH 8.0], 100 mM NaCl), supplemented with 10 μM PMSF (Sigma), 10 μM benzamidine (Sigma), 2 mM TCEP (Sigma), 1 mM $MgCl_2$, 10 μg/ml DNase I (Roche), and 100 μg/ml lysozyme (Sigma), and ruptured by sonification. After centrifugation, the supernatant was loaded on a Chelating Sepharose Fast Flow (Amersham) column, which had been charged with 200 mM nickel sulfate. The column was washed with buffer A supplemented with 15 mM imidazole. USP2 was eluted in one step with buffer A supplemented with 250 mM imidazole.

In a second purification step, the sample was applied to a size exclusion chromatography column (Superdex 75, HiLoad 26/60, Amersham) equilibrated with 45 mM potassium phosphate (pH 6.0), 300 mM NaCl. Fractions containing USP2 were diluted 1:3 in water and concentrated in an Amicon ultracentrifugation device (10 kDa cutoff) to concentrations ranging from 10 to 50 mg/ml. The concentrated protein was flash frozen as 20–50 μl aliquots in liquid nitrogen and stored at −80°C. The overall yield was up to 50 mg protein per one liter expression culture.

Human UCH-L3 was amplified from a cDNA library with the sense 5′-CTACTAGTGGCCATATGGAATCCATGGAGGGTCAACGC TGGCTG-3′ and the antisense primer 5′-CTCGAGCTCGAGCTATGC TGCAGAAAGAGCAAT-3′ and cloned into pET28a (Novagen) by using the restriction enzymes NcoI/XhoI. The encoded protein is full-length UCH-L3 without N- or C-terminal tags and was purified as described (Larsen et al., 1996). In the final purification step, UCH-L3 was eluted from the size-exclusion chromatography column (Superdex 75, HiLoad 26/60, Amersham) in 30 mM Tris (pH 8.0), 300 mM NaCl and treated as described for USP2. The overall yield was typically 40 mg pure protein per one liter expression culture.

Ubiquitin Preparation

Ubiquitin was amplified from a cDNA containing human ubiquitin precursor ubiquitin B (UBB) with the sense 5′-AAAAAAACATATGCA GATCTTCGTGAAGACCCTG-3′ and the antisense 5′-TTTGGATCCT CAGCCACCCCTCAGGCGCAGGACC-3′ and cloned into pET24a vector (Novagen) by using the restriction enzymes NdeI/BamHI. The plasmid encodes for mature human ubiquitin *1–76*, K48R without any N- or C-terminal tags, hereon referred to as "ubiquitin." Three C-terminal truncated ubiquitin mutants were generated with the antisense primers 5′-TTTGGATCCTCACCTCAGGCGCAGGAC CAGGTGC-3′, 5′-TTTGGATCCTCACAGGCGCAGGACCAGGTGCA GGG-3′, and 5′-TTTGGATCCTCAGCGCAGGACCAGGTGCAGGG TCG-3′. These plasmids encode for ubiquitin *1–74*, lacking residues *Gly75* and *Gly76*, ubiquitin *1–73*, lacking residues *Arg74*, *Gly75*, and *Gly76*, and ubiquitin *1–72*, lacking residues *Leu73* to *Gly76*.

Ubiquitin, ubiquitin *1–74*, ubiquitin *1–73*, and ubiquitin *1–72* were expressed and purified as described (Rajesh et al., 1999). The last purification step was a size-exclusion chromatography (Superdex 75, HiLoad 26/60, Amersham) in 50 mM Tris (pH 8), 50 mM NaCl. Ubiquitin-containing fractions were concentrated in Amicon ultracentrifugation devices (5 kDa cutoff), flash frozen in 50 μl aliquots, and stored at −80°C.

Prior to biophysical characterization of these proteins, the sample buffers were changed from 50 mM Tris (pH 8), 50 mM NaCl to 50 mM Tris-D11 (fully deuterated, Cambridge Isotope Laboratories) (pH 7.5), 100 mM NaCl in D_2O with desalting spin columns (Pierce). The samples were first analyzed by one-dimensional ^{1}H-NMR spectroscopy (DRX600, Bruker) and subsequently by differential scanning calorimetry (VP Capillary-DSC, MicroCal). Commercially available ubiquitin (Sigma U6253), which is purified from bovine thymus, was used as a reference. Please note that bovine ubiquitin is identical to heterologously expressed human ubiquitin *1–76*, with the exception of the K48R mutation.

Kinetic Methods

Kinetic analysis was performed at 22°C by using an Ultra microtiter plate reader (TECAN) with a 360 nm/465 nm filter pair. In a typical experiment, 10 μl assay buffer was transferred to a 384-well plate (Clinplate black, Labsystems) and mixed with 10 μl of enzyme and 10 μl of substrate solution. The final buffer was 50 mM Tris/HCl (pH 7.5), 1 mM EDTA, 5 mM DTE, 100 mM NaCl, 0.1% (w/v) CHAPS. The enzyme concentration was determined from its absorbance at 280 nm. Previous titration experiments with ubiquitin-aldehyde (Boston Biochem) have shown that our enzyme preparations were >95% active. Data analysis was done with Origin 6.1 (Microcal).

Kinetic parameters were determined for the fluorogenic substrates ubiquitin-AMC (ubiquitin C-terminally derivatized with fluorogenic 7-amido-4-methylcoumarin, Boston Biochem), RLRGG-AMC, and HLVLRLRGG-AMC (both Biosyntan). Initial velocities in triplicates were plotted versus substrate concentration ranging from 0 to 20 μM, and K_M and v_{max} were calculated in a nonlinear regression fit with the Michaelis-Menten equation $v = (v_{max} \times [S])/([S] + K_M)$. The k_{cat} was obtained from the equation $k_{cat} = v_{max}/[E_o]$, where $[E_o]$ is the total enzyme concentration. In these assays, the final enzyme concentration was 3 pM for UCH-L3 and 1.5 nM for USP2.

For determination of the inhibition constants K_i, UCH-L3 (1 pM enzyme) or USP2 (0.5 nM enzyme) were incubated with varying concentrations (0–100 μM) of inhibitor (ubiquitin, ubiquitin truncation mutants, and C-terminal peptide Ac-HLVLRLRGG-OH) in the assay buffer for 60 min at 22°C. Residual enzymatic activity was determined by measuring the rate of hydrolysis ubiquitin-AMC by USP2 (5 μM substrate) and UCH-L3 (0.5 μM substrate) in triplicate. The apparent inhibition constant for each enzyme-inhibitor pair was determined from the uninhibited rate (v_o) and inhibited rates (v_i) by plotting v_i/v_o versus the inhibitor concentration. In such a plot, the slope equals $1/K_{i(apparent)}$. For competitive inhibition, the inhibition constant is defined as $K_i = K_{i\ (apparent)}/(1 + [S]/K_M)$, where [S] is the concentration of ubiquitin-AMC. Please note that the competitive mechanism of inhibition has not been shown experimentally. In a competitive mechanism, inhibitor and substrate compete for the same binding site, which is most likely the case as ubiquitin-AMC and the inhibitor, ubiquitin and its deletion mutants, are almost identical molecules.

Complex Formation, Crystallization, and Data Collection

The USP2/ubiquitin complex was formed by mixing 40 μl USP2 (11.8 mg/ml in 15 mM potassium phosphate [pH 6.0], 100 mM NaCl, 25 mM DTT) and 20 μl ubiquitin (Sigma U6253, 10 mg/ml in H_2O demin) corresponding to a 1:2 molar ratio. Initial sparse matrix screens were set up at 23°C after incubation at 4°C overnight. By using an Oryx 6 crystallization robot (Douglas Instruments), 0.5 μl premade solution (Index screen, Hampton Research) was added to 0.5 μl of the protein complex in a modified microbatch format (D'Arcy et al., 2003). Crystals grew within 24 hr in eight out of 96 conditions. All these conditions contained polyethylene glycol or polyethylene glycol monomethyl ether as the primary precipitating agent. No crystals were obtained when identical crystallization trials were set up with either free USP2 or free ubiquitin. Analysis of crystals by SDS-PAGE showed the presence of both USP2 and ubiquitin (data not shown).

A crystal cryo-mounted directly from the first initial screen (200 mM $MgCl_2$, 100 mM Bis-Tris [pH 6.5], 25% w/v PEG 3350) initially diffracted to only 4 Å on a Nonius FR591 rotating anode operated at 5 kW equipped with a MAR345 imaging plate detector. In an attempt to improve the diffraction quality, we applied a simple, recently published dehydration protocol (Abergel, 2004). The same crystal was transferred to 10 μl of the crystallization solution supplemented with 30% glycerol as a cryoprotectant. During this process the crystal cracked. A single piece was isolated, placed in 10 μl of the

Table 3. Crystallographic Data and Refinement Statistics

Data Set Statistics	
Resolution limits (Å)	50.2–1.85 (1.93–1.85)
R_{sym} (%)[a]	6.1 (21.3)
I/σ(I)	16.1 (4.0)
Completeness (%)	95.5 (81.8)
Number of observations	116,236
Number of reflections	28,474
Crystal	
Space group	C2
a, b, c (Å)	106.9, 45.5, 76.4
α, β, γ (°)	90, 110, 90
Refinement Statistics	
Resolution (Å)	41.47–1.85 (1.97–1.85)
Number of reflections	28,473 (3923)
Completeness working + test set	95.5
Cutoff criteria F/σ(F)	0
R_{cryst}[b]	17.7% (22.9%)
R_{free}[b]	22.9% (26.4%)
Number of nonhydrogen atoms	
Protein atoms	3,128
Water molecules	160
Zinc ion	1
Bond length rmsd (Å)	0.016
Bond angles rmsd (°)	1.5
Ramachandron plot (core, allowed, generous) (%)	93.4, 6.0, 0.6

The values in parentheses correspond to the highest resolution shell.

[a] $R_{sym} = \Sigma|I - \langle I\rangle|/\Sigma I$, where I is the observed intensity, and <I> is the average intensity from multiple observations of symmetry-related reflections.

[b] $R_{cryst} = \Sigma||F_o| - |F_c||/\Sigma|F_o|$, where F_o and F_c are observed and calculated structure factors, respectively. R_{free} is the R factor calculated for a 5% subset of reflections selected at random.

same solution, and dehydrated for 30 min at 23°C. Then, the crystal was mounted and flash frozen again. This procedure lead to a significant improvement of the diffraction quality (maximum resolution 2.5 Å on FR591 generator), and spots could be observed up to 1.65 Å on a FR-E SuperBright generator operated at 2 kW equipped with a Saturn92 CCD detector (both Rigaku). Due to the small size of the detector (92 mm × 92 mm), its rectangular shape, and the low crystal symmetry, the completeness of the high-resolution data was acceptable only up to 1.85 Å, despite collecting data in three swipes at different 2τ, κ, and φ angles. Data sets were integrated and scaled with XDS (Kabsch, 1993) as part of the APRV package (Kroemer et al., 2004). For data collection statistics see Table 3.

Structure Determination and Refinement

The structure was determined by molecular replacement with Phaser (Storoni et al., 2004). Search models were taken from the PDB (ubiquitin, 1OGW; USP7, 1NBF chain C residues 211 to 533 without the 494 to 512 loop). One ubiquitin molecule and one USP7 catalytic domain could be placed in the asymmetric unit. To avoid clashes, several surface loops had to be removed. At this stage, the sequence of the model was changed to corresponding USP2 residues only in areas where the sequence alignment between USP2 and USP7 was unambiguous. Elsewhere, the sequence was changed to alanines. Starting from this modified model, 336 of 435 (359 USP2 and 76 ubiquitin residues) residues could be traced automatically in ARP/wARP (Perrakis et al., 1997), and an additional 53 residues could be placed manually with Main (Turk, 1992) for visual inspection and CNX (Accelrys) for refinement. The resulting model lacks 46 amino acids. For structure refinement statistics see Table 3. Figures were made in Pymol (DeLano Scientific, http://www.pymol.org/).

Supplemental Data

Supplemental Data include the description of an MAD experiment that was used for the determination of the metal bound to the zinc ribbon present in USP2 and are available online at http://www.structure.org/cgi/content/full/14/8/1293/DC1/.

Acknowledgments

We thank Drs. V. Quesada and C. Lopez-Otin (both University Oviedo, Spain) for making the complete multiple sequence alignment of human USPs available to us, P. Brunet-Lefeuvre for analyzing our protein samples by mass spectrometry and differential scanning calorimetry, Dr. P. Erbel for analyzing samples of recombinant ubiquitin by NMR (both Novartis Institutes for BioMedical Research, Switzerland), and Dr. E. Pohl for support at the Swiss Light Source (Paul Scherrer Insitute, Switzerland). All the authors of this manuscript are employees of Novartis Pharma, Novartis Institutes for Biomedical Research.

Received: April 10, 2006
Revised: June 11, 2006
Accepted: June 16, 2006
Published: August 15, 2006

References

Abergel, C. (2004). Spectacular improvement of X-ray diffraction through fast desiccation of protein crystals. Acta Crystallogr. D Biol. Crystallogr. *60*, 1413–1416.

Alberts, I.L., Nadassy, K., and Wodak, S.J. (1998). Analysis of zinc binding sites in protein crystal structures. Protein Sci. *7*, 1700–1716.

Amerik, A.Y., and Hochstrasser, M. (2004). Mechanism and function of deubiquitinating enzymes. Biochim. Biophys. Acta *1695*, 189–207.

Baron, A., Migita, T., Tang, D., and Loda, M. (2004). Fatty acid synthase: a metabolic oncogene in prostate cancer? J. Cell. Biochem. *91*, 47–53.

Cummins, J.M., and Vogelstein, B. (2004). HAUSP is required for p53 destabilization. Cell Cycle *3*, 689–692.

Buckle, A.M., Schreiber, G., and Fersht, A.R. (1994). Protein-protein recognition: crystal structural analysis of a barnase-barstar complex at 2.0-A resolution. Biochemistry *33*, 8878–8889.

Cummins, J.M., Rago, C., Kohli, M., Kinzler, K.W., Lengauer, C., and Vogelstein, B. (2004). Disruption of HAUSP gene stabilizes p53. Nature *428*, 1–2.

D'Arcy, A., Mac Sweeney, A., Stihle, M., and Haber, A. (2003). The advantages of using a modified microbatch method for rapid screening of protein crystallization conditions. Acta Crystallogr. D Biol. Crystallogr. *59*, 396–399.

Dang, L.C., Melandri, F.D., and Stein, R.L. (1998). Kinetic and mechanistic studies on the hydrolysis of ubiquitin C-terminal 7-amido-4-methylcoumarin by deubiquitinating enzymes. Biochemistry *37*, 1868–1879.

Graner, E., Tang, D., Rossi, S., Baron, A., Migita, T., Weinstein, L.J., Lechpammer, M., Huesken, D., Zimmermann, J., Signoretti, S., and Loda, M. (2004). The isopeptidase USP2a regulates the stability of fatty acid synthase in prostate cancer. Cancer Cell *5*, 253–261.

Hu, M., Li, P.W., Li, M.Y., Li, W.Y., Yao, T.T., Wu, J.W., Gu, W., Cohen, R.E., and Shi, Y.G. (2002). Crystal structure of a UBP-family deubiquitinating enzyme in isolation and in complex with ubiquitin aldehyde. Cell *111*, 1041–1054.

Hu, M., Li, P.W., Song, L., Jeffrey, P.D., Chernova, T.A., Wilkinson, K.D., Cohen, R.E., and Shi, Y.G. (2005). Structure and mechanisms of the proteasome-associated deubiquitinating enzyme USP14. EMBO J. *24*, 3747–3756.

Hu, M., Gu, L., Li, M.Y., Jeffrey, P.D., Gu, W., and Shi, Y.G. (2006). Structural basis of competitive recognition of p53 and MDM2 by HAUSP/USP7: implcations for the regulation of the p53-MDM2 pathway. Proc. Natl. Acad. Sci. USA *4*, 1–12.

Huang, K., Lu, W.Y., Anderson, S., Laskowski, M., and James, M.N.G. (1995). Water molecules participate in proteinase-inhibitor interactions: crystal-structures of Leu18, Ala18, and Gly18 variants

of turkey ovomucoid inhibitor third domain complexed with *Streptomyces griseus* proteinase B. Protein Sci. *4*, 1985–1997.

Janin, J. (1997). Specific versus non-specific contacts in protein crystals. Nat. Struct. Biol. *4*, 973–974.

Johnston, S.C., Larsen, C.N., Cook, W.J., Wilkinson, K.D., and Hill, C.P. (1997). Crystal structure of a deubiquitinating enzyme (human UCH-L3) at 1.8 angstrom resolution. EMBO J. *16*, 3787–3796.

Jones, S., and Thornton, J.M. (1996). Principles of protein-protein interactions. Proc. Natl. Acad. Sci. USA *93*, 13–20.

Kabsch, W. (1993). Automatic processing of rotation diffraction data from crystals of initially unknown symmetry and cell constants. J. Appl. Crystallogr. *26*, 795–800.

Krishna, S.S., and Grishin, N.V. (2005). The finger domain of the human deubiquitinating enzyme HAUSP is a zinc ribbon. Cell Cycle *3*, 1046–1049.

Kroemer, M., Dreyer, M.K., and Wendt, K.U. (2004). APRV—a program for automated data processing, refinement and visualization. Acta Crystallogr. D Biol. Crystallogr. *60*, 1679–1682.

Larsen, C.N., Price, J.S., and Wilkinson, K.D. (1996). Substrate binding and catalysis by ubiquitin C-terminal hydrolases: identification of two active site residues. Biochemistry *35*, 6735–6744.

Larsen, T.A., Olson, A.J., and Goodsell, D.S. (1998). Morphology of protein-protein interfaces. Structure *6*, 421–427.

Li, M.Y., Chen, D.L., Shiloh, A., Luo, J.Y., Nikolaev, A.Y., Qin, J., and Gu, W. (2002). Deubiquitination of p53 by HAUSP is an important pathway for p53 stabilization. Nature *416*, 648–653.

Li, M.Y., Brooks, C.L., Kon, N., and Gu, W. (2004). A dynamic role of HAUSP in the p53-Mdm2 pathway. Mol. Cell *13*, 879–886.

Nijman, S.M.B., Luna-Vargas, M.P.A., Velds, A., Brummelkamp, T.R., Dirac, A.M.G., Sixma, T.K., and Bernards, R. (2005). A genomic and functional inventory of deubiquitinating enzymes. Cell *123*, 773–786.

Perrakis, A., Sixma, T.K., Wilson, K.S., and Lamzin, V.S. (1997). wARP: improvement and extension of crystallographic phases by weighted averaging of multiple-refined dummy atomic models. Acta Crystallogr. D Biol. Crystallogr. *53*, 448–455.

Priolo, C., Tang, D., Brahamandan, M., Benassi, B., Sicinska, E., Ogino, S., Farsetti, A., Porrello, A., Finn, S., Zimmermann, J., et al. (2006). The isopeptidase USP2a protects human prostate cancer from apoptosis. Cancer Research *66*, in press.

Quesada, V., Diaz-Perales, A., Gutierrez-Fernandez, A., Garabaya, C., Cal, S., and Lopez-Otin, C. (2004). Cloning and enzymatic analysis of 22 novel human ubiquitin-specific proteases. Biochem. Biophys. Res. Commun. *314*, 54–62.

Quiocho, F.A., Wilson, D.K., and Vyas, N.K. (1989). Substrate-specificity and affinity of a protein modulated by bound water molecules. Nature *340*, 404–407.

Rajesh, S., Sakamoto, T., Iwamoto-Sugai, M., Shibata, T., Kohno, T., and Ito, Y. (1999). Ubiquitin binding interface mapping on yeast ubiquitin hydrolase by NMR chemical shift perturbation. Biochemistry *38*, 9242–9253.

Ratia, K., Saikatendu, K.S., Santarsiero, B.D., Barretto, N., Baker, S.C., Stevens, R.C., and Mesecar, A.D. (2006). Severe acute respiratory syndrome coronavirus papain-like protease: structure of a viral deubiquitinating enzyme. Proc. Natl. Acad. Sci. USA *103*, 5717–5722.

Rodier, F., Bahadur, R.P., Chakrabarti, P., and Janin, J. (2005). Hydration of protein-protein interfaces. Proteins *60*, 36–45.

Sheng, Y., Saridakis, V., Saridakis, F., Duan, S., Wu, T., Arrowsmith, C.H., and Frappier, L. (2006). Molecular recognition of p53 and MDM2 by USP7/HAUSP. Nat. Struct. Mol. Biol. *13*, 285–291.

Stein, R.L., Chen, Z.J., and Melandri, F. (1995). Kinetic studies of isopeptidase T: modulation of peptidase activity by ubiquitin. Biochemistry *34*, 12616–12623.

Storer, A.C., and Menard, R. (1994). Catalytic mechanism in papain family of cysteine peptidases. Methods Enzymol. *244*, 486–500.

Storoni, L.C., McCoy, A.J., and Read, R.J. (2004). Likelihood-enhanced fast rotation functions. Acta Crystallogr. D Biol. Crystallogr. *60*, 432–438.

Tsai, C.J., Lin, S.L., Wolfson, H.J., and Nussinov, R. (1997). Studies of protein-protein interfaces: a statistical analysis of the hydrophobic effect. Protein Sci. *6*, 53–64.

Turk, D. (1992). Weiterentwicklung eines programms für molekuelgraphik und elektrondichte-manipulation und seine anwendung auf verschiedene protein-strukturaufklärungen. PhD Thesis, Technische Universität, München.

Wilkinson, K.D., Laleli-Sahin, E., Urbauer, J., Larsen, C.N., Shih, G.H., Haas, A.L., Walsh, S.T.R., and Wand, A.J. (1999). The binding site for UCH-L3 on ubiquitin: mutagenesis and NMR studies on the complex between ubiquitin and UCH-L3. J. Mol. Biol. *291*, 1067–1077.

Westerik, J.O., and Wolfenden, R. (1972). Aldehydes as inhibitors of papain. J. Mol. Biol. *247*, 8195–8197.

Accession Numbers

The coordinates and structure factors are available at the Protein Data Bank (2HD5, RCSB038216).